

pubs.acs.org/Macromolecules Article

Programming Self-Assembly and Stimuli-Triggered Response of Hydrophilic Telechelic Polymers with Sequence-Encoded **Hydrophobic Initiators**

Adrian Moreno, Juan C. Ronda, Virginia Cádiz, Marina Galià, Virgil Percec,* and Gerard Lligadas*



Cite This: Macromolecules 2020, 53, 7285-7297



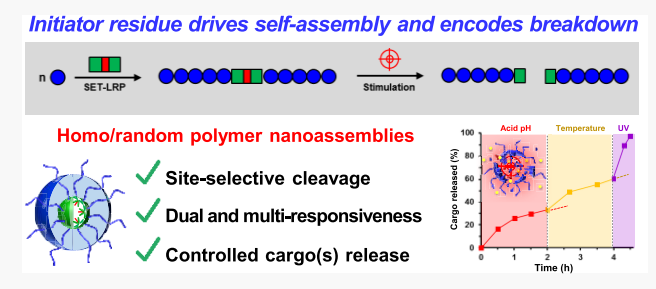
ACCESS

III Metrics & More

Article Recommendations

s Supporting Information

ABSTRACT: A recent communication from our laboratory demonstrated that the presence of a small hydrophobic initiator residue (core) in water-soluble telechelic dibromo homopolymers can drive their self-assembly in aqueous solution into micelle-like nano-objects in which polymer chains adopt a folded conformation. Centered on the use of site-selective cleavable difunctional initiators, we demonstrate herein that this approach offers bottom-up and facile access to multistimuli-sensitive nanostructures for effective cargo delivery. Here, we first report the synthesis of homopolymers and copolymers encoding hydrophobicity and cleavable sites in their



initiator residue in a precise sequence by single-electron transfer living radical polymerization (SET-LRP) from oligo(ethylene glycol) (macro)monomers. Employing a designed acid pH/UV light dual-cleavable initiator integrating a 2-nitroresorcinol diacetal sequence enabled on-demand middle-chain scission of the polymer chains and hence rapid/slow breakdown of the assemblies upon appropriate stimulation. Additionally, the possibility to interrogate binary co-delivery systems sequence-encoded with complimentary reactivity with combinatorial stimuli not only allows for fine-tuning the guest molecule release kinetics but also provides a mechanism to achieve control of their release behavior when different cargos are loaded.

INTRODUCTION

The great wealth of fascinating self-assembly behavior observed in amphiphilic macromolecular structures comes from the covalent linking of dissimilar hydrophilic, or water-soluble, and hydrophobic constituents within a single polymer chain and so forcing them to live next to each other. Like their smallmolecule surfactant analogues, the solution self-assembly of these macromolecular amphiphiles can lead to a variety of nanoaggregates, such as spherical micelles, vesicles, and wormlike structures, to reduce energetically unfavorable hydrophobic/water interactions. Such morphologies have captivated the attention across many scientific disciplines from materials science to biology, aroused by their remarkable property of long-term stability and high loading capacity for guest species. Macromolecular amphiphiles are even more attractive when endowed with the ability to sense and respond to different stimuli, such as temperature, light, pH, and gases, among others, in a prescribed fashion. 5-9 A review in this field, however, will reflect that decades of fundamental research have mostly revolved around well-defined amphiphilic block copolymers (ABCPs) prepared by living radical polymerization (LRP) techniques. However, is there any chance to encode homopolymers, which are more readily synthesized, with selfassembling behavior?

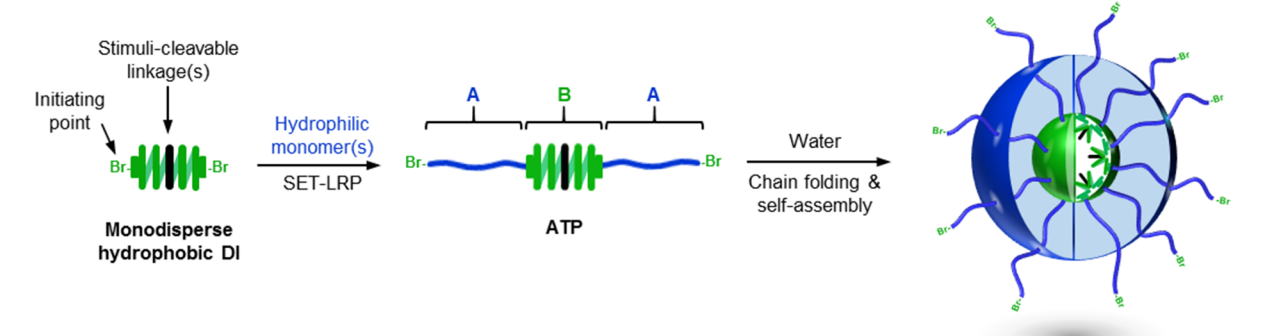
To address this question, intensive studies have been undertaken in recent years to design and synthesize simplified ABCP-mimicking systems based on single monomeric units, i.e., homopolymers, containing both hydrophilic and hydrophobic moieties. ^{10,11} Like amphiphilic AB or ABA copolymers, amphiphilic homopolymers prepared from properly designed monomers 12-15 or alternatively by using modular modifications to a repeating unit structure in a postpolymerization modification approach $^{16-19}$ have been shown to self-assemble into well-defined nanostructures making them promising materials for applications in which aqueous solution-assembly is a requirement, e.g., drug loading and release, sensing, and catalysis. 12,20 In addition to the monomer-induced approach, self-associative fully hydrophilic homopolymers prepared by the LRP of universal water-soluble monomers, such as triethylene glycol acrylate, N-isopropyl acrylamide, and oligo-(ethylene glycol) methyl ether acrylate (OEGA), are attractive alternative options. 21-25 In such a special class of amphiphilic homopolymers, aggregation in aqueous medium is driven by the presence of hydrophobic end groups, i.e., end-groupinduced approach, introduced through chain transfer agents or

Received: June 15, 2020 Revised: July 29, 2020 Published: August 18, 2020





A Self-assembly of ATPs by "hydrophobic-core-induced" approach



Stimuli-breakable ATP nanoassemblies with DI residues forming hydrophobic core

B Sequence-encoded hydrophobic and control SET-LRP initiators used herein

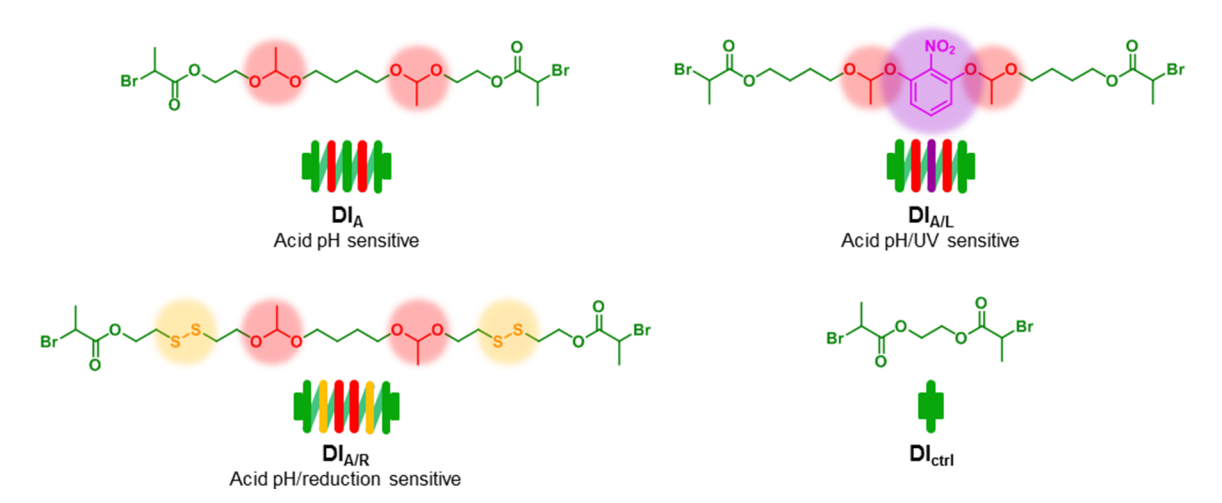


Figure 1. Programming hydrophilic telechelic polymers with self-associative character and stimuli-response. (a) Schematic representation of ATPs prepared from DI by SET-LRP and their hydrophobic-core-induced self-assembly to form micelle-like assemblies with the DI residue forming the hydrophobic core. (b) Chemical structures and symbol codes for the hydrophobic and flexible stimuli-cleavable difunctional initiators (DIs) used herein. Color code: blue as hydrophilic and water-soluble, green as hydrophobic and water-insoluble, red as acidic pH-sensitive acetal linkages, purple as UV-light-sensitive 2-nitroresorcinol-derived linkages, and orange as reduction-sensitive disulfide linkages.

initiators containing aromatic or aliphatic groups. However, to our knowledge, no interest was reported on molecular engineering at the center of fully hydrophilic homo/copolymers with the primary goal of introducing amphiphilicity. In this sense, by taking advantage of single-electron transfer living radical polymerization (SET-LRP), 26-28 we have recently proposed a simple design strategy for associative telechelic polymers (ATPs), that is, hydrophobicity to program self-assembly steams from the initiator residue precisely positioned within the two hydrophilic arms of a homotelechelic polymer (Figure 1A). ²⁹ Although this ABA framework may resemble conventional amphiphilic triblock copolymers, it is incorrect to consider that because in these ATPs the central block B has a monodisperse nature and is very small. Our findings led us to propose that the tiny core unit, despite representing a low volume fraction of the homopolymer, drives fully hydrophilic telechelic polymer chains to self-assemble into micelle-like nanoassemblies in which polymer chains adopt a folded conformation, i.e., "hydrophobic-core-induced" approach (Figure 1A). More importantly, the careful design of the initiator residue may also provide a useful approach for the control of their degradation, 30 which could be amenable to the

generation of stimuli-responsive drug carriers. In a preliminary communication, a showcase acidic pH sensitive hydrophobic and flexible α -haloester difunctional initiator (DI_A in Figure 1B) was used to deliver biocompatible OEGA-derived ATPs capable of spontaneously organizing into micelle-like nanoassemblies upon dissolution in water. Delightfully, the site-specific pH-triggered cleavage of any of the two acetal linkages in the symmetric polymeric arrangement dramatically modifies the amphiphilic balance; i.e., acetal hydrolysis splits the polymer chain into two equally sized fragments, further resulting in the breakdown of nanoassemblies.

Given the possibility to rationally design and synthesize telechelic dibromo homopolymers from sequence-encoded DIs with single- $^{32-34}$ and multistimuli-responsiveness 35 using LRP techniques, 36 we speculated that the hydrophobic-coreinduced approach could represent an efficient bottom-up strategy to produce smart ATP-based nanocarriers. In this article, a pH/UV-light dual-type cleavable α -haloester difunctional initiator $\mathrm{DI}_{\mathrm{A/L}}$, in which the structure is shown in Figure 1B, integrating a 2-nitroresorcinol acetal (NRA) sequence inserted between the two initiating points allowed for the

A SET-LRP synthesis and self-assembly of ATPs1-3

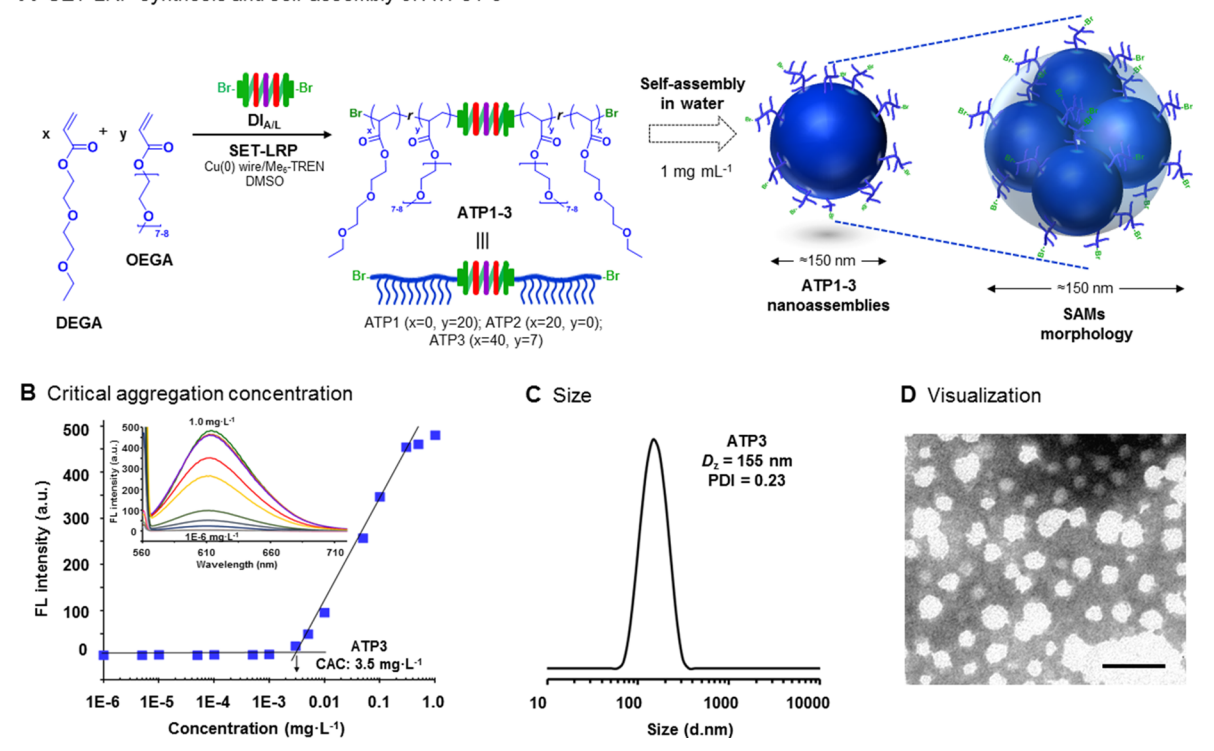


Figure 2. Use of the sequence-encoded hydrophobic initiator $DI_{A/L}$ to program self-assembly and stimuli-triggered response of hydrophilic telechelic homo/random ATPs. (A) Schematic representation for the SET-LRP synthesis of APT1-3 from DEGA and OEGA using the difunctional initiator $DI_{A/L}$ and subsequent assembly of pH/UV dual stimuli-responsive nanoassemblies by direct dissolution in water at 1 mg·mL⁻¹. (B) Fluorescence intensity of NR at 625 nm (λ_{exc} = 550 nm) vs ATP3 concentration (mg·mL⁻¹). (C) Representative DLS size distribution by intensity measurement and (D) TEM image with negative staining using phosphotungstic acid of an aqueous colloidal dispersion of ATP3 self-assembled by direct dissolution in water at 1 mg·mL⁻¹. Scale bar in panel (D) is 100 nm.

Table 1. Characterization of the ATPs and Their Self-Assembly Parameters in Aqueous Media

ATP^a	monomer(s)	initiator	stimuli-response	conv. ^b (%)	$M_{\rm n}^{\ c} \ ({\rm kDa})$	$M_{\rm w}/M_{\rm n}^{\ c}$	DIR ^d (wt %)	D_z^e (nm)	PDI^e	$CAC^{g} (mg \cdot L^{-1})$
1	OEGA	$\mathrm{DI}_{\mathrm{A/L}}$	pH/UV	90	9.5	1.24	5.3	167	0.19	2.9
2	DEGA	$\mathrm{DI}_{\mathrm{A/L}}$	pH/UV	86	4.3	1.23	11.6	345	0.40	3.5
								165 ^f	0.23^{f}	
3	OEGA/DEGA	$\mathrm{DI}_{\mathrm{A/L}}$	pH/UV/T	89	12.1	1.23	4.1	155	0.23	3.1
4	OEGA	$\mathrm{DI}_{\mathrm{ctrl}}$		93	10.8	1.18	1.6	6	0.23	nd
5	OEGA	DI_A	pН	94	9.4	1.21	3.5	110	0.13	0.7
6	OEGA	$DI_{A/R}$	pH/reduction	89	9.1	1.26	6.2	196	0.21	1.3

"Polymerization conditions: OEGA = 0.5 mL, DMSO = 0.25 mL, and $[OEGA]_0/[DI]_0/[Me_6-TREN]_0 = 20/1/0.2$ (for ATP1,4–6), DEGA = 0.5 mL, DMSO = 0.25 mL, and $[DEGA]_0/[DI_{A/L}]_0/[Me_6-TREN]_0 = 20/1/0.2$ (for ATP2), and OEGA = 0.2 mL, DEGA = 0.4 mL DMSO = 0.25 mL, and $[DEGA]_0/[OEGA]_0/[OEGA]_0/[DI_{A/L}]_0/[Me_6-TREN]_0 = 40/7/1/0.2$ (for ATP3). In all cases, 4.5 cm hydrazine-activated Cu(0) wire (20-gauge diameter) was used. Determined by 1 H NMR. Determined by GPC in THF using PMMA standards. Weight fraction of the hydrophobic initiator residue in the whole hydrophilic ATP. Determined by DLS in water at 25 °C. Measurement conducted at 0 °C. Critical aggregation concentration determined by fluorescence spectroscopy using Nile Red as a probe.

preparation of a series of di(ethylene glycol) ethyl ether acrylate (DEGA)- and OEGA-derived telechelic homo- and random copolymers via SET-LRP. The ability of the newly formed ATPs to self-assemble and encapsulate model hydrophobic compounds in aqueous media was investigated to emphasize the effect of both the initiator residue and polymer chain on the self-assembly. Further, the dual fast-slow responsiveness of the NRA unit, precisely inserted within the telechelic polymer, has been investigated pursuing to intelligently deliver encapsulated hydrophobic model compounds in response to acidic pH and UV-light exposure either applied individually (steady or intermittently), simultaneously, or successively. Finally, it has been demonstrated that the use

of binary mixtures of various loaded nanoassemblies, programmed in the synthetic step with stimuli-responsive sequences allowing for complementary reactivity, has great potential as a tool for building smart platforms for cocktail drug delivery.

■ RESULTS AND DISCUSSION

Synthesis of Homo- and Random ATPs. Synthesis of homo/random ATP1-3 with pH/UV dual stimuli-breakable hydrophobic core units is depicted in Figure 2A. Cu(0)-mediated SET-LRP is a versatile synthetic tool that enables the preparation of vinylic polymers with precisely defined complex molecular architectures and chain-end fidelity. Hence,

A

$$Br \mapsto Br$$
 $Br \mapsto Br$
 $Br \mapsto B$

Figure 3. Synthetic strategies for the stimuli-cleavable difunctional initiators used in this work. Color code: green as hydrophobic and water-insoluble, red as acid pH-, purple as UV-light-, and orange as reduction-sensitive linkages.

using the difunctional initiator $\mathrm{DI}_{\mathrm{A/L}}$ in which an NRA unit bridges the two α -haloester-type initiating sites, the SET-LRP technique was employed herein to polymerize the nontoxic OEGA ($M_{\mathrm{n}}=480~\mathrm{g\cdot mol^{-1}}$) and DEGA monomers, aiming to provide two well-defined symmetric homopolymers showing different water solubilities (ATP1 and ATP2, respectively) (Table 1).

Poly(OEGA) is a highly hydrophilic homopolymer, which is soluble in water at any temperature up to 100 °C, whereas poly(DEGA) demonstrates a low critical solution temperature (LCST) close to 0 °C, and therefore is hydrophobic at ambient temperature. As previously reported, DI_{A/L} was synthesized following a two-step procedure, in which 1,4-butanediol vinyl ether is first esterified with 2-bromopropionyl bromide and subsequently reacted with 2-nitroresorcinol in the presence of pyridinium p-toluenesulfonate (PPTS) (Figure 3A).

In principle, the NRA sequence can be chemo (acid hydrolysis)- and photo (UV to near-infrared regime)-cleaved to generate the corresponding alcohols, 2-nitroresorcinol, and acetaldehyde (Figure S1).35,38 In both experiments, the total degree of polymerization (DP) was set as 20 (10 for each two initiating sites). Under classic SET-LRP conditions, ^{26,39} i.e., a homogeneous reaction mixture in DMSO using a Cu(0) wire catalyst and tris[2-(dimethylamino)ethyl]amine (Me6-TREN) ligand, the two homopolymerizations proceeded rapidly and most of the vinylic monomer was consumed after 2 h (monomer conversion of ≈90%, Table 1). GPC characterization of the final dialyzed products revealed monomodal GPC curves corresponding to $M_{\rm n}^{\rm GPC}$ = 9.5 kDa $(M_{\rm w}/M_{\rm n}$ = 1.24) and $M_{\rm n}^{\rm GPC}$ = 4.3 kDa $(M_{\rm w}/M_{\rm n}$ = 1.23) for ATP1 and ATP2, respectively, suggesting that both monomers polymerized successfully from DI_{A/L} and that SET-LRPs were controlled (Table 1).

As a representative example, the kinetics of the polymerization reaction of DEGA was monitored by ¹H NMR. GPC was employed to follow the evolution of the molecular weight distribution. As can be seen in Figure S2, the polymerization achieved near 90% conversion in 120 min. It can be seen that the molar mass of the polymer increased monotonically and

agreed well with the theoretical values calculated from monomer conversion assuming 100% initiator efficiency (Figure S2, right panel). Moreover, the evolution of $ln([M]_0/[M])$ versus reaction time showed a linear correlation (left panel). Such a kinetic behavior is consistent with a constant concentration of active species throughout the entire reaction, the absence of major side reactions, and consequently a well-controlled radical polymerization. Based on the successful synthesis of telechelic homopolymers, a random copolymerization of both monomers ([DEGA]₀/[OEGA]₀/ $[DI_{A/L}]_0/[Me_6\text{-TREN}]_0 = 40/7/1/0.2)$ was performed under similar conditions, aiming at building up a nontoxic thermoresponsive copolymer ATP3 with LCST close to body temperature. 40-42 The random copolymerization reached 90% after 2 h, as proven by ¹H NMR spectroscopy, and GPC analysis confirmed the presence of a monomodal copolymer distribution with $M_n^{\text{GPC}} = 12.1 \text{ kDa}$ and $M_w/M_n = 1.23$ (Table 1). As expected, the ¹H NMR spectrum of ATP3 in CDCl₃ (Figure S3, lower spectrum), a good solvent for both the core unit and copolymer chains, showed characteristic peaks associated with the repeating unit structure, i.e., $\delta_{13,18} = 4.2$ ppm, and middle-chain initiator residue, i.e., $\delta_{9.7}$ = 6.7 and 5.4 ppm. However, pleasingly, in D₂O, a selective solvent to the hydrophilic poly(DEGA)-r-(OEGA) backbone (upper spectrum), the initiator residue peaks were strongly attenuated suggesting that hydrophobic initiator residues were bent, aggregated together, and confined in the polar hydrophilic solution with the telechelic polymer chains being forced to adopt a folded conformation (Figure 1A). These measurements can be interpreted to indicate some associative character of the ATPs investigated in the present study.

With three ATPs in our hands, we used ATP3 as a representative example to survey whether the NRA sequence, inserted between the two poly(DEGA)-*r*-(OEGA) arms, can sense environmental acid pH and UV-light exposure conditions in the dissolved state and undergo cleavage with the subsequent split of the symmetric polymeric chain into two equally sized fragments.³¹ In good agreement with the behavior observed in a homologous buildup of poly(methyl acrylate),³⁵ GPC traces revealed that the molar mass of the copolymer

suffered a remarkable decrease from 9.5 down to 4.2 kDa upon acidic pH exposure for 1 h (50 mg of the polymer in 2 mL of THF/0.1 M TFA solution) (compare black and red traces in Figure S4). The same polymer, dissolved in THF, was subjected to UV-light irradiation at 365 nm for 1 h. Also in this case, GPC analysis of the resulting polymer revealed a shift of the GPC trace to longer elution times compared with the parent polymer as a result of the UV photolysis of NRA units (purple trace in Figure S4). The above presented results prompted us to study in detail the aggregation of the synthesized polymers in aqueous solution in more detail.

Self-Assembly Study. Subsequent to the synthesis and characterization of ATPs, their self-organization in water was investigated by a combination of fluorescence spectroscopy, dynamic light scattering (DLS), and transmission electron microscopy (TEM). The second evidence for self-assembly was obtained from critical aggregation concentration (CAC) studies conducted by tracking the fluorescence emission intensity of Nile Red (NR) as a function of the ATP concentration. As a representative example, Figure 2B depicts how the fluorescence intensity at 617 nm rapidly increases above a certain concentration of ATP3. Apparent low CAC values ranging from 3.5 to 2.7 mg·L⁻¹ were determined from the intersection of two straight lines, therefore confirming the ability of the synthesized polymers to formulate assemblies with good stability against dilution above a certain concentration. The CAC values increased with an increase of the DEGA content, indicating that higher hydrophilicity of the polymer chain favors the formation of aggregates.

Next, we became curious about the size and morphology of the formed aggregates. Initially, we focused our attention on the study of OEGA containing polymers, i.e., ATP1 and ATP3. In line with our previous study, ²⁹ both systems were expected to be amphiphilic in character with a large solubility difference between the two polymer arms, either poly(OEGA) or poly(DEGA)-r-(OEGA), and the monodisperse sequencedefined DI_{A/L} initiator residue. Hence, the corresponding aqueous polymer solutions, prepared by direct dissolution at a concentration much greater than the CAC (1 mg·mL⁻¹), were studied. In both cases, we noted completely transparent colloid dispersions at 25 °C. DLS measurements confirmed the presence of nanoaggregates with an average hydrodynamic diameter (D_h) value of ca. 160 nm (167 nm for ATP1 and 155 nm for ATP3), which is a much larger particle size than that expected for simple core-shell micelles (Figure S5 and Figure 2C). Conversely, the DLS analysis of equivalent solutions prepared in CHCl₃ showed the presence of polymer chains rather than self-assembled nanostructures (Figure 4A).

In stark contrast, no aggregates were detected for telechelic poly(OEGA) containing an ethylene glycol derived core prepared from a control DI (DI_{ctrl} in Figure 1B) in both solvents (Figure 4B). These observations support that the presence of a monodisperse hydrophobic and flexible initiator residue plays a crucial role for nanoassembly formation when two fully hydrophilic chains are attached at their extremities. Subsequently, TEM was used to visualize ATP nanoassembly morphology. In the dried state, ATP1 and ATP3 created nonuniform nanoparticles due to their nonregular spherical shape according to TEM imaging (Figure 2D and Figure S6). It is worth mentioning that the average $D_{\rm h}$ of the nanoaggregates measured by DLS (>150 nm) was much bigger than the size estimated by TEM measuring the average diameter of more than 25 single particles (<80 nm). Although small

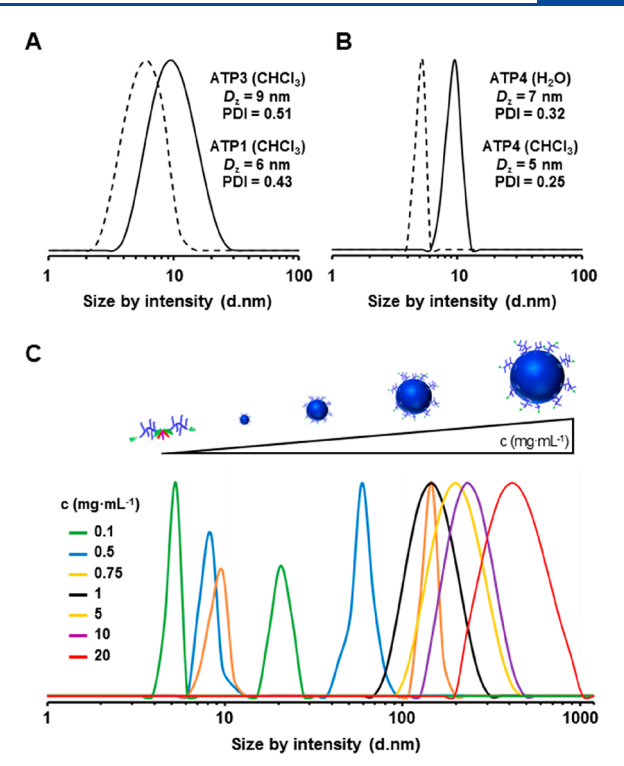


Figure 4. DLS analysis of ATPs in various solvents and concentrations. (A) DLS curves of ATP1 (dashed line) and ATP3 (solid line) solutions in CHCl₃ (1 mg·mL⁻¹, 25 °C), (B) DLS curves of ATP4 in CHCl₃ (dashed line) and H₂O (solid line) at 1 mg·mL⁻¹, 25 °C, and (C) DLS curves of ATP3 nanoassemblies in aqueous solution as a function of the polymer concentration (pH 7.4, 25 °C).

discrepancies in soft assembly size between DLS and TEM can be attributed to the fact that measurements are conducted in different states, 43 such a huge difference might suggest that ATPs 1 and 3 self-assemble at a concentration of 1 mg·mL⁻¹ to form nanogel-like spherical aggregated micelles (SAMs) with many hydrophobic pockets that are interconnected by loose hydrophilic chains within each SAM rather than simple core shell micelles. Note that the total length of the telechelic polymer is much shorter than the half of D_h determined by DLS. This feature has been reported to occur in many other macromolecular amphiphilic systems with poly(ethylene glycol) and poly(N-isopropylacrylamide) hydrophilic segments. ^{23,44–49} The nature of this particles allows deep penetration of water, which is consistent with the abovementioned much smaller average particle sizes as measured from TEM than from DLS as well as with the attenuation of the ¹H NMR signals of hydrophilic oligo(oxyethylene) side chains when comparing the spectra recorded in D_2O and $CDCl_3$ (Figure S3). Further, concentration-dependent DLS measurements on ATP3 support the presence of nanogellike SAMs because they demonstrated that larger aggregates, i.e., aggregates of aggregates, formed when the polymer concentration was higher than 1.0 mg·mL⁻¹, e.g., 197 and 420 nm at 5 and 20 mg·mL⁻¹, respectively (Figure 4C). In contrast, DLS measurements at lower concentrations revealed a decrease in aggregates size, which suggests a transition from multicore SAM nanoassemblies, to simple spherical micelles, and then finally to random coils upon dilution. These observations indicated that polymer concentrations have a significant effect on the self-assembled nanostructures.

Next, we focused our attention on the self-assembly behavior of ATP2, a telechelic homopolymer containing two poly-(DEGA) arms with LCST close to 0 °C. This polymer formed in water (1 mg·mL⁻¹) a turbid emulsion-like suspension rather than a transparent colloid dispersion. As expected, DLS analysis at room temperature demonstrated the presence of nanoparticles with increased size of ca. 350 nm and much broader distribution (PDI = 0.34) compared with ATP1 and ATP3 (Figure S7, blue line). TEM allowed imaging the spherelike large aggregates formed at room temperature (Figure S8). However, decreasing the temperature of the solution to 5 °C, a value close to the LCST of poly(DEGA), did significantly change the size of the formed aggregates toward smaller nanoaggregates (345 versus 165 nm) with lower PDI (0.34 versus 0.21) (Figure S7, red line). At low temperature, many of the poly(DEGA) chains change from a hydrophobic state to a swollen hydrophilic state, and this transition decreases hydrophobic effects, further driving the assembly of the polymer by folding of the symmetric telechelic architecture.⁵⁰ This viewpoint, but in a completely opposite way, was also confirmed by examining the temperature-response behavior of the random copolymer ATP3 in aqueous solution (Figure 5, vide infra for details). This is powerful evidence that not only hydrophobicity of the initiator residue but also hydrophilicity of the polymer chain dominates the self-assembly of the ATPs studied herein. In view of the previous discussions, we anticipated pH/UV dual stimuli-responsiveness for all the

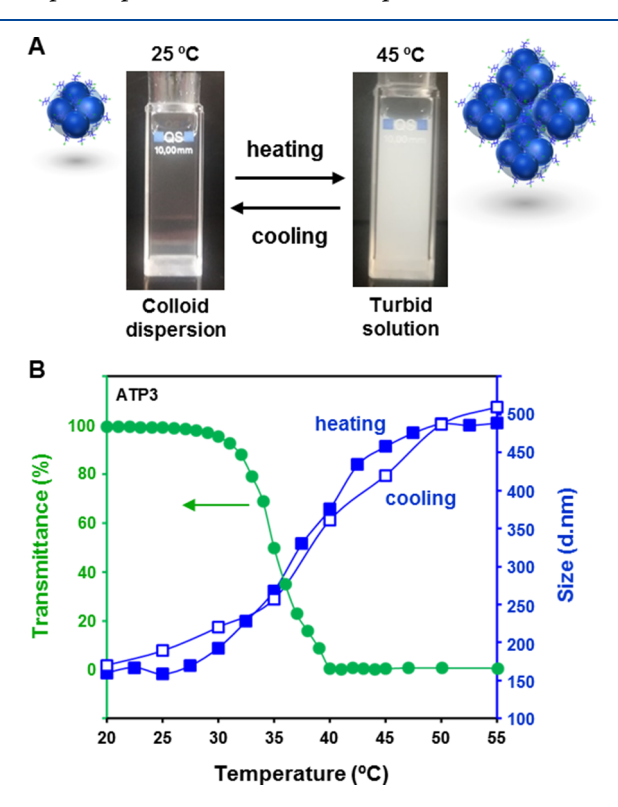


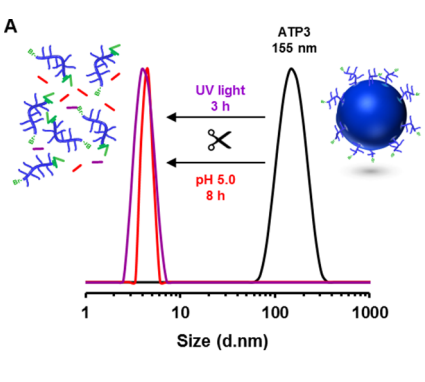
Figure 5. Thermoresponsive behavior of ATP3 nanoassemblies. (A) Digital images captured at 25 and 45 $^{\circ}$ C show the temperature responsiveness of ATP3 nanoassemblies. (B) Transmitted laser light intensity (green circles, measured by UV) and hydrodynamic diameter (filled and open blue squares, measured by DLS) vs temperature for ATP3 self-assembled in water by direct dissolution (1 mg·mL⁻¹). Digital images captured at 25 and 45 $^{\circ}$ C show the temperature responsiveness of ATP3 nanoassemblies.

synthesized ATP nanoassemblies whose hydrophobic core sequence contains an NRA unit. Even so, we chose the nontoxic random copolymeric system ATP3 for subsequent investigations because in addition it was programmed with thermoresponsiveness.

Thermoresponsive Behavior of ATP3 Nanoassemblies. As mentioned above, it was visualized that the transparent colloid dispersion of random copolymer ATP3 in water (1 mg·mL⁻¹) became opaque when the sample was heated at 45 °C (Figure 5A). However, following a temperature decrease back to room temperature, the turbid solution became transparent again. This so-called thermoresponsive behavior is a common feature of random co-polymers of DEGA and OEGA, rending them attractive for cargo delivery especially in medical applications. 40-42,50 Thermoresponsive polymers become insoluble when the temperature increases above a critical temperature, i.e., LCST, due to the coil-to-globule transition.⁵¹ The LCST of such random copolymers can be precisely programmed to be at a specific temperature near human body temperature by varying the comonomer composition in the feed. 42 The thermoresponsive behavior of ATP3 nanoassemblies was studied in more detail using temperature-dependent UV/vis turbidimetry and DLS measurements (Figure 5B). Upon heating, the transmittance of the colloid dispersion decreased, reaching a 50% decrease in optical transmittance, i.e., LCST, at 35 °C. A light transmittance decrease from 99 to 1% was observed when temperature increased from 20 to 55 °C (circles in Figure 5B). Temperature evolution of D_h was also monitored throughout the heating process (filled blue squares). In the lower temperature range, the $D_{\rm h}$ values were close to the initial value (155 nm) and only increased slightly. However, the values dramatically increased in the higher temperature range. Overall, the D_h of the assembled nanoparticles increased from 155 up to around 500 nm at 55 °C.

These results can be explained as follows. At low temperature, the poly(DEGA)-r-(OEGA) chains in the corona/inside the swelled nanoassemblies exist in random coil conformations due to the intermolecular hydrogenbonding interactions between the polymer and water molecules. When the temperature increases and passes through the critical LCST, co-polymer chains shrank to a globular structure because the intermolecular hydrogen bonds between the polymer chains and water collapse, resulting in the aggregation of collapsed dehydrated chains. Consequently, ATP3 nanoaggregates, i.e., SAMs with multicore structures, tended to form aggregates of aggregates with larger sizes in the higher temperature range. DLS monitoring of the cooling process confirmed the reversibility of the ATP3 thermoresponsive behavior (open blue squares).

pH/UV Dual Stimuli-Response of ATP3 Nanoassemblies. It was anticipated that the cleavage of the multiple NRA units located at the hydrophobic cores of ATP3 nanoassemblies can trigger their breakdown as a result of middlechain cleavage. Thus, their colloidal stability in acidic environments was examined by DLS. An important size decrease was observed after incubating ATP3 nanoassemblies (1 mg·mL⁻¹) at pH 5.0 for 8 h, implying the decomposition of the nanoaggregates caused by the disruption of the original hydrophobic/hydrophilic balance via acid hydrolysis of the multiple acetal linkages (compare black and red traces in Figure 6A).^{53,54} Interestingly, size evolution over 8 h of acidic incubation was discontinuous. During the first 5 h, the D_h of



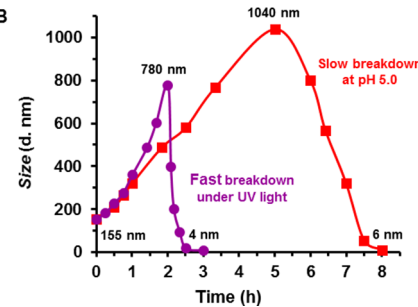


Figure 6. pH- and UV-light-triggered breakdown of self-assembled ATP3. (A) DLS data of ATP3 self-assembled in water before (black trace) and after applying pH = 5.0 (8 h, red trace) or UV-light irradiation (3 h at λ = 365 nm, purple trace) treatments. (B) DLS profiles showing the evolution of size during the breakdown process of ATP3 nanoassemblies under acidic conditions (red trace) and exposure to UV light (purple trace).

the ATP3 nanoassemblies increased progressively from 155 up to 1040 nm, but thereafter, the particles suffered an abrupt decline in size. After long-time acidic incubation, a size distribution centered at 6 nm was observed, hinting toward mostly water-soluble copolymer unimers of half molecular weight being present in solution (red line in Figure 6B). These results confirm the occurrence of a slow and sustained pH-triggered breakdown of the nanoassemblies and suggest that the disassembly process obeys a swelling-to-crack mechanism. To test UV-responsiveness, the same colloid dispersion was illuminated at 365 nm. Also, in this case, the original nanoassembly population disappeared, while a new population with $D_{\rm h}=4$ nm appeared (Figure 6B). However, the photolysis disassembly process was much faster than acidic hydrolysis

since a size distribution with $D_{\rm h}$ below 10 nm could be found after less than 3 h of steady irradiation.

ATP3 nanoassemblies also swell and increase in diameter prior to irreversible breakdown, although the process was much faster in this case. As a control, the size of SAMs had no alteration after 6 h without stimulation (data not shown). Therefore, the interest in these nanoassemblies resides in the fact that not only they can break down in response to two relevant internal/external stimuli but also their disassembly rates under the effect of each of the two stimuli are very different.

Next, to assess the possibility of utilizing these nano-objects as smart containers to transport and release hydrophobic guests in a controlled fast/slow manner, we investigated their encapsulation/release capabilities under a variety of environmental conditions. Thus, the fluorescent dye NR was selected as the model molecule to be encapsulated into the ATP3 nanoassemblies by hydrophobic interactions since it is insoluble and does not fluoresce in water, while it can exhibit a high fluorescence intensity once encapsulated into hydrophobic pockets.⁵⁵ The NR loading and release characteristics were studied by fluorescence spectroscopy. The loading amount and encapsulation efficiency were 7.5 and 86.0%, respectively. Upon stimulation with either acidic pH or UV exposure, a decrease of the fluorescence intensity occurred, indicating that NR precipitated from the aqueous solution as a result of the scission of NRA units (Figures S9 and S1). The NR release profile from polymer nanoassemblies, calculated from the fluorescence decrease divided by the primary fluorescence intensity, showed important changes with pH value alteration (Figure 7A).

At pH 7.0, there was a slow release of about 18% of NR from the loaded nanoassemblies over a period of 7 h. However, at lower and more biologically relevant pH values, the release of cargo dramatically accelerated due to a quicker acid hydrolysis of the pH-sensitive acetal linkers. For example, at pH 6.0, about 50% of the cargo was released after 7 h, while more than 90% of the loaded NR was released on the same timescale at pH 5.0. In accordance with the DLS results, the UV-boosted NR release displayed an abrupt and faster kinetic profile than under any of the studied acidic environments (squares in Figure 7B). A near quantitative NR release could be achieved upon steady UV irradiation on the timescale of 2.5 h. Furthermore, light is an attractive stimulus because of the flexibility it offers in terms of the spatiotemporal control. ⁵⁶

Intermittent

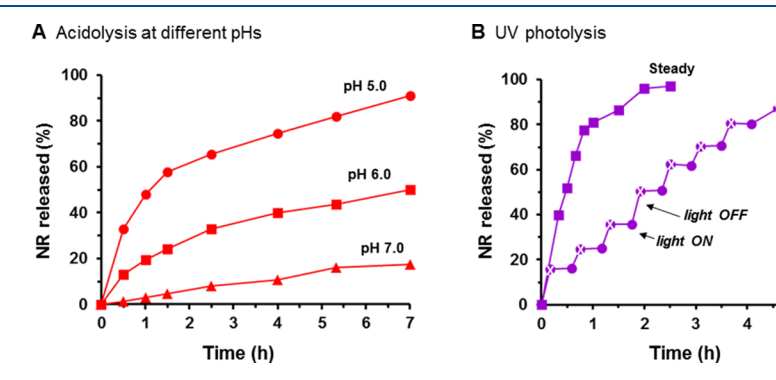


Figure 7. Single-stimuli-triggered cargo release from ATP3-NR nanoassemblies. (A) NR release profile from ATP3 nanoassemblies in aqueous solution upon applying pH 7.0 (triangles), 6.0 (squares), or 5.0 (circles) as a function of time. (B) NR release profile from ATP3 nanoassemblies in aqueous solution upon applying either steady (squares) or intermittent (irradiation time: 10 min, circles) UV-light irradiation (λ = 365 nm) as a function of exposure time.

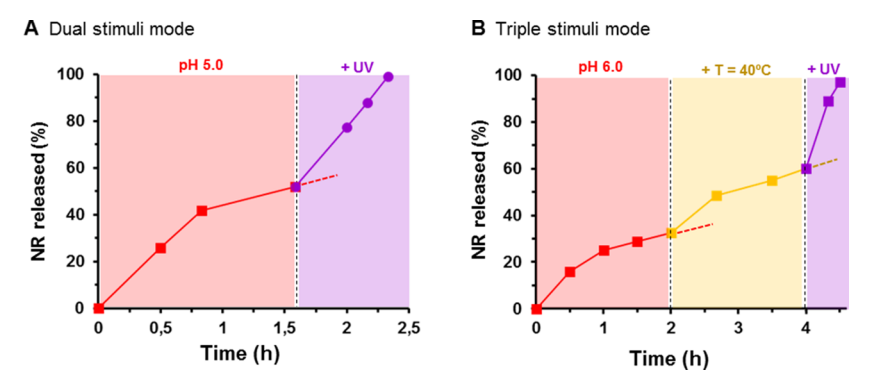


Figure 8. Multistimuli-triggered cargo release from ATP3-NR nanoassemblies. (A) Dual stimuli study: NR release profile from ATP3 nanoassemblies in aqueous solution upon applying pH 5.0 followed by UV-light irradiation (λ = 365 nm). (B) Triple stimuli study: NR release profile from ATP3 nanoassemblies in aqueous solution upon applying pH 6.0, then increasing the temperature up to 40 °C, and finally irradiating with UV-light (λ = 365 nm).

Hence, we subsequently investigated how the release of NR could be temporally regulated by modulating the UV illumination using intermittent light and dark exposure for alternating 10/25 min on/off sequences. In this case, the decay of fluorescence intensity occurred only during light-on periods (Figure S10). As can be seen in Figure 7B denoted by the circles, approximately 15% of NR was released after the first period of UV stimulation. Dark exposure at this point resulted in a nearly complete discontinuation of the release process. On re-exposing the mixture after 35 min (dark period of 25 min), the release process was restored with nearly the same rate. Repeated light-on and light-off cycles, equating to a total exposure time of 130 min, resulted in an NR release level comparable with that obtained by steady UV-light illumination (squares in Figure 7B). Overall, these results demonstrate that the simple ATP3 system allows encapsulated hydrophobic cargo(s) to be released in aqueous solution either rapidly (burst release) by UV- or ultimately NIR-light exposure³⁸ or slowly (sustained release) upon applying acidic pH.

Multistimuli-Response of ATP3 Nanoassemblies. The existence of a thermoresponsive poly(DEGA)-r-(OEGA) hydrophilic corona and pH/UV dual stimuli-responsive cores in ATP3 nanoassemblies makes the investigation of their multiresponsiveness extremely attractive for fine-tuning their stability toward precision drug delivery.⁵⁷ As schematically represented in Figure S11, multiple possibilities to regulate cargo delivery/release behaviors are envisioned when varying one or various of these parameters (temperature, pH, and UV exposure) individually (steady or intermittently), simultaneously, or successively. As shown in Figure 8A, a representative dual-stimuli release mode experiment demonstrated that the NR release profile from ATP3 nanoassemblies under acidic conditions (pH = 5.0) can be suddenly accelerated by incorporating UV exposure. As a result, whereas the NR release rate was slowing down gradually under an acidic environment, reaching a level <60% after 100 min, under co-triggered conditions (acidic pH + UV), NR release accelerated and was nearly complete after a 40 min period of UV exposure at pH 5.0.

Therefore, the combination of the two stimuli might be used to conduct intermittent light-mediated pulsative administration treatments during sustained therapies in biologically relevant acidic compartments.⁵⁸ Next, to demonstrate the potential of cooperative stimuli strategies, acidic pH, temperature, and UV exposure were successively applied in a cumulative fashion to

an aqueous solution of NR-loaded nanoassemblies of ATP3. Although temperature does not trigger disassembly, we hypothesized that structural changes induced by the temperature signal above the LCST, in turn, would also activate NR release. 59 As observed in Figure 8B, the NR release amount was only about 30% after 120 min at pH 6.0 at room temperature. However, a faster response was observed when the solution was heated up at 40 °C, showing that the temperature condition has an obvious regulating effect on drug release. The cumulative percentage after 120 min at 40 °C was about 60%. Then, the aqueous solution of the remaining NRloaded nanoassemblies was subjected to UV exposure. Under co-triggered conditions, i.e., pH, temperature, and UV, an ultrafast and quantitative release of the remaining guest molecules took place in less than 20 min of exposure. These observations indicate that ATP3 nanoassemblies may be particularly interesting to develop therapeutic drug delivery systems taking advantage of the sequential as well as synergistic combined use of internal stimuli (i.e., acidic pH and temperature) and external stimuli (i.e., UV-light or ultimately NIR irradiation) signals.

ATP-Based Co-Delivery Systems to Fine-Control the Release of Loaded Cargo(s). Considering the rich side variability possible for stimuli-responsive DIs, 31-35 we speculated that the use of binary mixtures of ATP nanoassemblies programmed with complementary reactivity could be an advantageous platform to fine-control the release of loaded cargo(s). Herein, we present two proof-of-concept experiments for the use of ATP-based co-delivery systems. First of all, we synthesized two additional sequence-encoded hydrophobic SET-LRP initiators DIA and DIA/R, in which structures are shown in Figure 1B, following previously reported procedures (Figure 3B,C, respectively).35 SET-LRP initiator DIA, by integrating acetal linkages, was conceived to further deliver ATPs sensitive only to acidic pH values, whereas the preparation of DI_{A/R} pursued pH/reduction dual stimuli degradation; i.e., it contains both acetal and disulfide linkages. Note that pH and reductive environments have received increasing attention owing to their advantages in overcoming multiple biological barriers.⁶⁰ The originality of these initiators relies not only on their individual stimuliresponsiveness but also on the possibilities that their combinations with the pH/UV dual-sensitive initiator DI_{A/L} offer.³⁵ Next, the newly synthesized initiators were used to deliver two additional OEGA-derived ATPs containing acidic

A Schematic of the cargo loading and release via different triggering steps

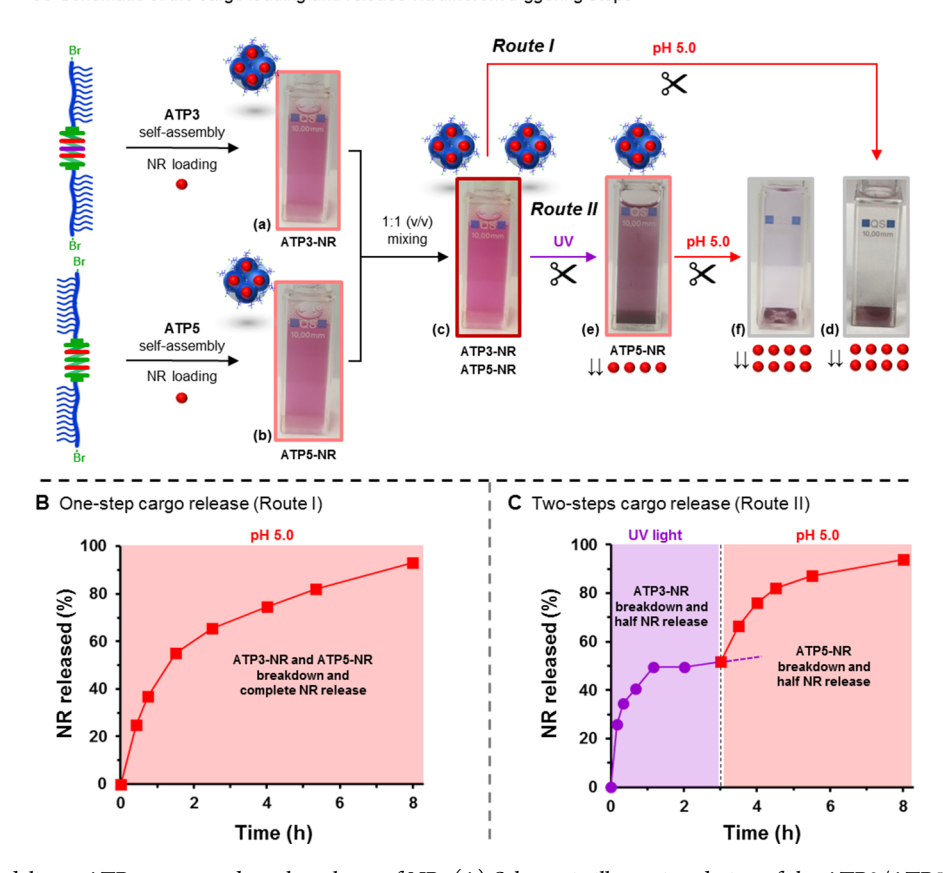


Figure 9. Use of a co-delivery ATP system to dose the release of NR. (A) Schematic illustration design of the ATP3/ATP5 co-delivery system to dose the release of NR: (i) NR-loaded ATP3 and ATP5 nanoassemblies, i.e., ATP3-NR and ATP5-NR, were individually prepared in aqueous solution (pH 7.4) by the solvent evaporation method; (ii) both solutions were mixed at a 1:1 (v/v) ratio to deliver a binary mixture of loaded nanoassemblies; and (iii) the NR release from the co-delivery system was investigated following two procedures: acidic pH treatment (pH 5.0 for 8 h at 25 °C) (route I) or sequential UV exposure (λ = 365 nm, 3 h) and acidic pH treatment (pH 5.0 for 5 h at 25 °C) (route II). (B) NR release profile from the ATP3/ATP5 co-delivery system in aqueous solution upon applying pH 5.0 at 25 °C (route I) as a function of time. (C) NR release profile from the ATP3/ATP5 co-delivery system in aqueous solution upon applying sequentially UV exposure (λ = 365 nm, 3 h) and acidic pH treatment (pH 5.0 for 5 h at 25 °C) (route II) as a function of time. Digital images (a)—(f) show color changes through the different steps.

pH-sensitive (ATP5) and acidic pH/reduction dual-sensitive (ATP6) functionalities positioned at the center of the polymer chain. Both ATPs were easily prepared by SET-LRP under strictly identical reaction conditions (catalyst, ligand, solvent, monomer, DP) to those of ATP1 (Table 1). As expected, SET-LRP reactions proceeded in a controlled fashion and afforded well-defined telechelic polymers. Furthermore, the resulting telechelic homopolymers were shown to form well-defined selfassembled nanoaggregate structures in aqueous medium with remarkable stability upon dilution (Table 1 and Figure S12). Delightfully, the results of DLS measurements pointed toward the possibility to address the sequential disassembly of selected binary mixtures of these nanoassemblies, i.e., ATP3/ATP5 and ATP3/ATP6, by rationally exerting the proper two stimuli (see Figure S13 and related text discussion). According to these promising results, our first showcase experiment aimed to precisely dose the release of NR, loaded in the self-assembly step, into both pH/UV dual-sensitive ATP3 and pH-sensitive ATP5 nanoassemblies (Figure 9A). Importantly, after mixing the two solutions at 1:1 (v/v), no precipitates were observed, which means that NR remained loaded inside the nanoassemblies (see digital images (a)-(c) in Figure 9A). Encouragingly, different profiles were obtained for the NR release from the co-delivery system after receiving pH (route I)

or sequential UV/pH (route II) stimuli (Figure 9B,C, respectively).

As can be seen in digital images (c) and (d) captured after each step of route I, the characteristic bright red color of the ATP3-NR/ATP5-NR mixture disappeared while vast red precipitates of NR were observed at the bottom of the cuvette after 8 h of incubation at pH 5.0. Fluorescence spectroscopy measurements revealed that a sustained NR release took place in one step under these conditions (Figure 9B). Hence, near quantitative NR release occurred (93%) because both types of nanoassemblies are prone to break down under acidic conditions due to the presence of the acid-sensitive core. On the other hand, a two-step release process was obtained by successively exerting UV exposure and acidic pH stimuli because, under these conditions, a sequential breakdown of ATP3-NR and ATP5-NR nanoassemblies took place (Figure 9C). Gratifyingly, the NR release process only reached about 50% under photolysis conditions due to the selective breakdown of the ATP3-NR nanoassemblies containing NRA units. However, when medium pH turned acidic (pH 5.0), the release process immediately reactivated and reached a level of 94% because of the hydrolytic disassembly of the remaining ATP5-NR nano-objects. Digital images (c), (e), and (f) in Figure 9A are consistent with these observations.

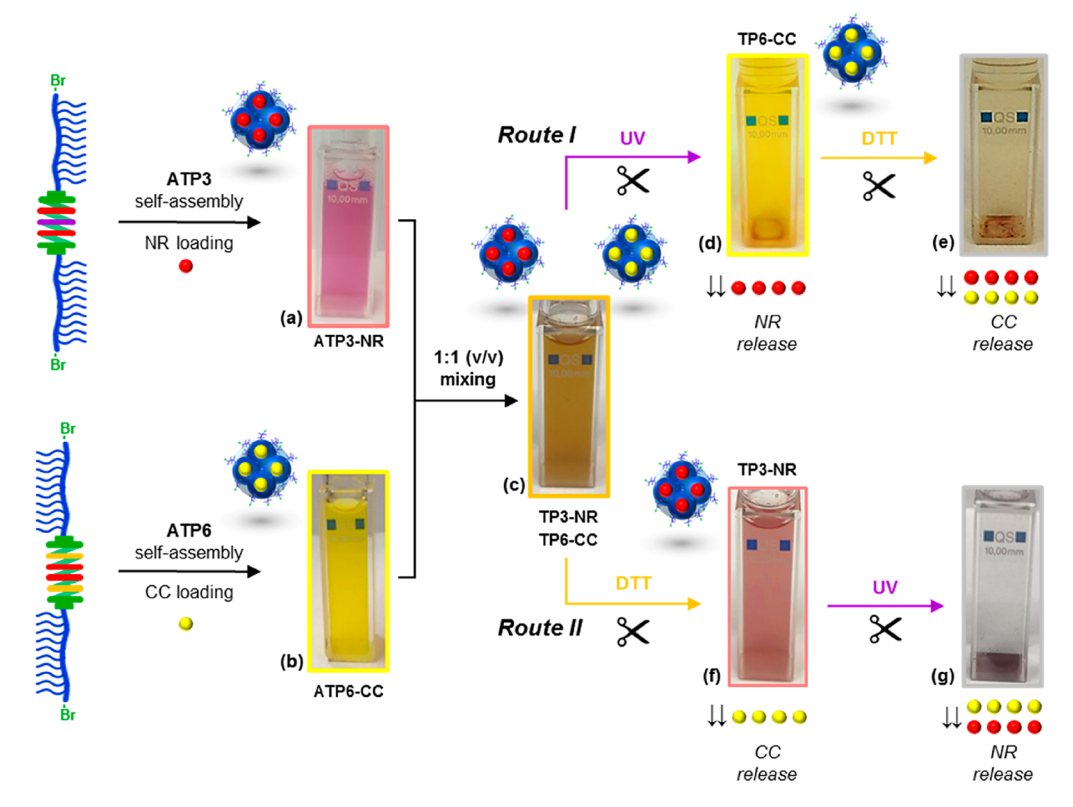


Figure 10. Use of a co-delivery ATP system to individually release different loaded cargos. Schematic illustration design of the ATP3/ATP6 co-delivery system to individually and sequentially release NR/CC: (i) NR-loaded ATP3 and CC-loaded ATP6 nanoassemblies, i.e., ATP3-NR and ATP6-CC, were individually prepared in aqueous solution (pH 7.4) by the solvent evaporation method; (ii) both solutions were mixed at a 1:1 (v/v) ratio to deliver a binary mixture of loaded nanoassemblies; and (iii) the sequential release of both dyes from the co-delivery system was investigated following two procedures: sequential UV exposure (λ = 365 nm, 3 h) and reductive treatment (0.1 M DTT, 5 h) (route I) or sequential reductive treatment (0.1 M DTT, 5 h) and UV exposure (λ = 365 nm, 3 h) (route II). Digital images (a)–(g) show color changes through the different steps.

To further demonstrate the great potential of combining different ATPs, we also attempted to address the release of different dyes (cocktail-type system) by using mixtures of nanoassemblies programmed with complementary reactivities. NR, with a characteristic red color in nonpolar environments, and curcumin (CC), giving a bright yellow color in nonpolar environments, were used as model dyes with the purpose of using vivid color changes to monitor the individual controlled release of both hydrophobic dyes from a co-delivery system based on ATP3 and ATP6 nanoassemblies (Figure 10). Briefly, we first prepared a 1:1 (v/v) mixture of ATP3-NR and ATP6-CC nanoassemblies by directly mixing the two colloid dispersions. After mixing the two solutions, a mixed color was obtained but no precipitates were observed, which means that both NR and CC were still entrapped inside the nanoassemblies after mixing (see digital images (a)-(c) in Figure 10).

After a first step of UV illumination for 2 h (route I), the brownish aqueous solution turned bright yellow and vast red precipitates of NR were observed since only ATP3-NR nanoassemblies broke down (see digital image (d) in Figure 10, route I). Only after the addition of DTT, ATP5-CC nanoassemblies were progressively destroyed, which led to the release of CC. Accordingly, the vivid yellow colored solution was hardly detected since both dyes are insoluble in aqueous solution in the absence of nanocarriers (see image (e) in Figure 10, route I). The above results indicate that the release of NR from ATP3 and CC from ATP5 were independent of

each other by applying UV-reduction sequential stimulation. It is worth mentioning that the release of the two guest molecules could be also achieved in reverse order by applying first reductive conditions and subsequently UV exposure (route II). However, the color changing in this case was not as intense (see digital images (c), (f), and (g) in Figure 10, route II). Indeed, the simultaneous release of NR and CC could be activated under acidic conditions as both systems are pHsensitive. In this case, a one-step progressive decoloration of the solution was observed (data not shown). These results further prove that the release behavior of two cargos can be controlled separately by the selection of appropriate ATPs and stimulation. Therefore, ATP co-delivery systems based on nontoxic monomers are worth exploring for creating nanoscale templates for advanced biomedical applications based on intracellular trafficking of drug cocktails. ⁶¹ Research in this line will be reported in a forthcoming publication.

CONCLUSIONS

Telechelic homopolymers with hydrophobic initiator residues and hydrophilic arms can directly self-organize in water to form micelle-like nanoaggregates in which polymer chains adopt a folded conformation.²⁹ Herein, we extend this approach to the elaboration of site-selective middle-chain cleavable ATP systems with the aim to control disassembly and kinetics of cargo release. First, homo- and random symmetric telechelic copolymers encoding hydrophobicity and responsiveness in their initiator residue sequences were synthesized

from biocompatible DEGA and OEGA vinyl monomers. Using Cu(0)-mediated SET-LRP, an acid pH/UV-light-sensitive monodisperse hydrophobic sequence was incorporated into the center of fully hydrophilic chains, resulting in a selfassembly process in aqueous solution that drives the synthesis of micelle-like aggregates with a clearly defined dual response. A combination of NMR, GPC, fluorescence spectroscopy, DLS, and TEM was first used to demonstrate that the driving force for self-assembly into nanocontainers capable of encapsulating hydrophobic guest molecules is provided by the presence of a testimonial hydrophobic core (<5 wt % of the overall polymer mass). These nanoassemblies possess a core encoding a sequence-defined cleavage pattern that can be disintegrated either rapidly, upon exposure of UV-light to conduct burst or pulsatile release of encapsulated cargos, or slowly through sustained cleavage of acetal linkages under acidic conditions. In this case, cargo release was slow and sustained but highly dependent on variation in pH. Indeed, the random copolymerization approach was used to endow the resulting nanoassemblies with thermoresponsive behavior allowing further fine-tuning the cargo release mode. We also demonstrated that co-delivery systems designed by combination of ATPs programmed with complementary reactivities, i.e., UV-light/acid pH and UV-light/reduction, will find great potential in applications in which precise control over drug cocktails is a requirement. The wide range of difunctional and multifunctional initiators and hydrophilic vinylic monomers accessible by SET-LRP makes the future of this facile accessible drug-delivery platform very promising for future studies. We expect to expand soon this approach to the area of biobased polymers using innovative biobased water-soluble monomers.62 as well as vinylic sugar-based monomers.63,64

ASSOCIATED CONTENT

Supporting Information

The Supporting Information is available free of charge at https://pubs.acs.org/doi/10.1021/acs.macromol.0c01400.

Materials, experimental procedures, characterization techniques, and additional data (proposed mechanism for the dual cleavage of NRA sequence, kinetics for ATP2 synthesis, ¹H NMR analysis of ATP3, GPC analysis of ATP3 mid-chain cleavage, additional DLS curves and TEM images for ATP1–3, fluorescence spectra recorded during selected NR-release experiments, schematic of multistimuli-responsive capabilities of ATP3 nanoassemblies, self-assembly study of ATPs 5 and 6, and DLS analysis during the selective breakdown of mixtures of nanoassemblies) (PDF)

AUTHOR INFORMATION

Corresponding Authors

Virgil Percec — Roy & Diana Vagelos Laboratories, Department of Chemistry, University of Pennsylvania, Philadelphia, Pennsylvania 19104-6323, United States; ⊚ orcid.org/0000-0001-5926-0489; Email: percec@sas.upenn.edu

Gerard Lligadas — Laboratory of Sustainable Polymers,
Department of Analytical Chemistry and Organic Chemistry,
University Rovira i Virgili, Tarragona 43007, Spain; Roy &
Diana Vagelos Laboratories, Department of Chemistry,
University of Pennsylvania, Philadelphia, Pennsylvania 19104-6323, United States; orcid.org/0000-0002-8519-1840;
Email: gerard.lligadas@urv.cat

Authors

Adrian Moreno — Laboratory of Sustainable Polymers,
Department of Analytical Chemistry and Organic Chemistry,
University Rovira i Virgili, Tarragona 43007, Spain
Juan C. Ronda — Laboratory of Sustainable Polymers,
Department of Analytical Chemistry and Organic Chemistry,
University Rovira i Virgili, Tarragona 43007, Spain
Virginia Cádiz — Laboratory of Sustainable Polymers,

Department of Analytical Chemistry and Organic Chemistry, University Rovira i Virgili, Tarragona 43007, Spain Marina Galia – Laboratory of Sustainable Polymers,

Marina Galià — Laboratory of Sustainable Polymers,
Department of Analytical Chemistry and Organic Chemistry,
University Rovira i Virgili, Tarragona 43007, Spain;
orcid.org/0000-0002-4359-4510

Complete contact information is available at: https://pubs.acs.org/10.1021/acs.macromol.0c01400

Notes

The authors declare no competing financial interest.

ACKNOWLEDGMENTS

Spanish Ministerio de Ciencia, Innovación y Universidades through project MAT2017-82669-R (to G.L. and J.C.R) and FPI grant BES-2015-072662 (to A.M.) and the Serra Hunter Programme of the Government of Catalonia (to G.L.) are acknowledged for supporting and funding this work. V.P. gratefully acknowledges support from the National Science Foundation Grants DMR-1066116, DMR-1807127 and the P. Roy Vagelos Chair at the University of Pennsylvania. Dr. Mathieu J.-L. Tschan is thanked for an inspiring discussion on co-delivery systems.

REFERENCES

- (1) Bates, F. S.; Fredrickson, G. H. Block Copolymers-Designer Soft Materials. *Phys. Today* **1999**, 52, 32–38.
- (2) Mai, Y.; Eisenberg, A. Self-Assembly of Block Copolymers. Chem. Soc. Rev. 2012, 41, 5969–5985.
- (3) Epps, T. H., III; O'Reilly, R. K. Block Copolymers: Controlling Nanostructure to Generate Functional Materials Synthesis, Characterization, and Engineering. *Chem. Sci.* **2016**, *7*, 1674–1689.
- (4) Smart, T.; Lomas, H.; Massignani, M.; Flores-Merino, M. V.; Perez, L. R.; Battaglia, G. Block Copolymer Nanostructures. *Nano Today* **2008**, *3*, 38–46.
- (5) Mura, S.; Nicolas, J.; Couvreur, P. Stimuli-Responsive Nanocarriers for Drug Delivery. *Nat. Mater.* **2013**, *12*, 991–1003.
- (6) Liu, X.; Hu, D.; Jiang, Z.; Zhuang, J.; Xu, Y.; Guo, X.; Thayumanavan, S. Multi-Stimuli-Responsive Amphiphilic Assemblies through Simple Postpolymerization Modifications. *Macromolecules* **2016**, *49*, 6186–6192.
- (7) Zhang, Q.; Lei, L.; Zhu, S. Gas-Responsive Polymers. *ACS Macro Lett.* **2017**, *6*, 515–522.
- (8) Ma, N.; Li, Y.; Xu, H.; Wang, Z.; Zhang, X. Dual Redox Responsive Assemblies Formed from Diselenide Block Copolymers. *J. Am. Chem. Soc.* **2010**, *132*, 442–443.
- (9) Mabire, A. B.; Brouard, Q.; Pitto-Barry, A.; Williams, R. J.; Willcock, H.; Kirby, N.; Chapman, E.; O'Reilly, R. K. CO2/pH-Responsive Particles with Built-In Fluorescence Read-Out. *Polym. Chem.* **2016**, *7*, 5943–5948.
- (10) Zhang, J.; Liu, K.; Müllen, K.; Yin, M. Self-Assemblies of Amphiphilic Homopolymers: Synthesis, Morphology Studies and Biomedical Applications. *Chem. Commun.* **2015**, *51*, 11541–11555.
- (11) Vasilevskaya, V. V.; Govorun, E. N. Hollow and Vesicle Particles from Macromolecules with Amphiphilic Monomer Units. *Polym. RevPolym Rev.* **2019**, *59*, 625–650.

- (12) Mane, S. R.; Rao, N. V.; Chaterjee, K.; Dinda, H.; Nag, S.; Kishore, A.; Sarma, J. D.; Shunmugam, R. Amphiphilic Homopolymer Vesicles as Unique Nano-Carriers for Cancer Therapy. *Macromolecules* **2012**, *45*, 8037–8042.
- (13) Mane, S. R.; Rao, N. V.; Shunmugam, R. Reversible pH- and Lipid-Sensitive Vesicles from Amphiphilic Norbornene-Derived Thiobarbiturate Homopolymers. ACS Macro Lett. 2012, 1, 482–488.
- (14) Wang, Y.; Alb, A. M.; He, J.; Grayson, S. M. Neutral Linear Amphiphilic Homopolymers Prepared by Atom Transfer Radical Polymerization. *Polym. Chem.* **2014**, *5*, 622–629.
- (15) Savariar, E. N.; Aathimanikandan, S. V.; Thayumanavan, S. Supramolecular Assemblies from Amphiphilic Homopolymers: Testing the Scope. *J. Am. Chem. Soc.* **2006**, *128*, 16224–16230.
- (16) Kubo, T.; Easterling, C. P.; Olson, R. A.; Sumerlin, B. S. Synthesis of Multifunctional Homopolymers *via* Sequential Post-Polymerization Reactions. *Polym. Chem.* **2018**, *9*, 4605–4610.
- (17) Kubo, T.; Bentz, K. C.; Powell, K. C.; Figg, C. A.; Swartz, J. L.; Tansky, M.; Chauhan, A.; Savin, D. A.; Sumerlin, B. S. Modular and Rapid Access to Amphiphilic Homopolymers via Successive Chemoselective Post-Polymerization Modification. *Polym. Chem.* **2017**, *8*, 6028–6032.
- (18) He, H.; Liu, B.; Wang, M.; Vachet, R. W.; Thayumanavan, S. Sequential Nucleophilic "Click" Reactions for Functional Amphiphilic Homopolymers. *Polym. Chem.* **2019**, *10*, 187–193.
- (19) Ramireddy, R. R.; Prasad, P.; Finne, A.; Thayumanavan, S. Zwitterionic Amphiphilic Homopolymer Assemblies. *Polym. Chem.* **2015**, *6*, 6083–6087.
- (20) Sandanaraj, B. S.; Demont, R.; Thayumanavan, S. Generating Patterns for Sensing Using a Single Receptor Scaffold. *J. Am. Chem. Soc.* **2007**, *129*, 3506–3507.
- (21) Du, J.; Willcock, H.; Patterson, J. P.; Portman, I.; O'Reilly, R. K. Self-Assembly of Hydrophilic Homopolymers: A Matter of RAFT End Groups. *Small* **2011**, *7*, 2070–2080.
- (22) Patterson, J. P.; Cotanda, P.; Kelley, E. G.; Moughton, A. O.; Lu, A.; Epps, T. H., III; O'Reilly, R. K. Catalytic Y-Tailed Amphiphilic Homopolymers-Aqueous Nanoreactors for High Activity, Low Loading SCS Pincer Catalysts. *Polym. Chem.* **2013**, *4*, 2033–2039.
- (23) Liu, T.; Tian, W.; Zhu, Y.; Bai, Y.; Yan, H.; Du, J. How Does a Tiny Terminal Alkynyl End Group Drive Fully Hydrophilic Homopolymers to Self-Assemble Into Multicompartment Vesicles and Flower-Like Complex Particles? *Polym. Chem.* **2014**, *5*, 5077–5088
- (24) Patterson, J. P.; Kelley, E. G.; Murphy, R. P.; Moughton, A. O.; Robin, M. P.; Lu, A.; Colombani, O.; Chassenieux, C.; Cheung, D.; Sullivan, M. O.; Epps, T. H., III; O'Reilly, R. K. Structural Characterization of Amphiphilic Homopolymer Micelles Using Light Scattering, SANS, and Cryo-TEM. *Macromolecules* **2013**, *46*, 6319–6325.
- (25) Fan, L.; Lu, H.; Zou, K.; Chen, J.; Du, J. Homopolymer Vesicles with a Gradient Bilayer membrane as Drug Carriers. *Chem. Commun* **2013**, *49*, 11521–11523.
- (26) Lligadas, G.; Grama, S.; Percec, V. Single-Electron Transfer Living Radical Polymerization Platform to Practice Develop and Invent. *Biomacromolecules* **2017**, *18*, 2981–3008.
- (27) Anastasaki, A.; Nikolaou, V.; Nurumbetov, G.; Wilson, O.; Kempe, K.; Quinn, J. F.; Davis, T. P.; Whittaker, M. R.; Haddleton, D. M. Cu(0)-Mediated Living Radical Polymerization: a Versatile Tool for Materials Synthesis. *Chem. Rev.* **2016**, *116*, 835–877.
- (28) Anastasaki, A.; Nikolaou, V.; Haddleton, D. M. Cu(0)-Mediated Living Radical Polymerization: Recent Highlights and Applications: a Perspective. *Polym. Chem.* **2016**, *7*, 1002–1026.
- (29) Moreno, A.; Ronda, J. C.; Cádiz, V.; Galià, M.; Lligadas, G.; Percec, V. pH-Responsive Micellar Nanoassemblies from Water-Soluble Telechelic Homopolymers Endcoding Acid-Labile Middle-Chain Groups in Their Hydrophobic Sequence-Defined Initiator Residue. ACS Macro Lett. 2019, 8, 1200–1208.
- (30) Zhang, Q.; Koa, N. R.; Oh, J. K. Recent Advances In Stimuli-Responsive Degradable Block Copolymer Micelles: Synthesis And

- Controlled Drug Delivery Applications. Chem. Commun 2012, 48, 7542–7552.
- (31) Delplace, V.; Nicolas, J. Degradable Vinyl Polymers for Biomedical Applications. *Nat. Chem.* **2015**, *7*, 771–784.
- (32) Fritze, U. F.; Craig, S. L.; von Delius, M. Disulfide-Centered Poly(methyl acrylates): Four Different Stimuli to Cleave a Polymer. *J. Polym. Sci., Part A: Polym. Chem.* **2018**, *56*, 1404–1411.
- (33) Lee, M. E.; Gungor, E.; Armani, A. M. Photocleavage of Poly(methyl acrylate) with Centrally Located *o*-Nitrobenzyl Moiety: Influence of Environment on Kinetics. *Macromolecules* **2015**, *48*, 8746–8751.
- (34) Peles-Strahl, L.; Sasson, R.; Slor, G.; Edelstein-Pardo, N.; Dahan, A.; Amir, R. J. Utilizing Self-Immolative ATRP Initiators To Prepare Stimuli-Responsive Polymeric Films from Nonresponsive Polymers. *Macromolecules* **2019**, *52*, 3268–3277.
- (35) Moreno, A.; Ronda, J. C.; Cádiz, V.; Galià, M.; Lligadas, G.; Percec, V. SET-LRP from Programmed Difunctional Initiators Encoded with Double Single-Cleavage and Double Dual-Cleavage Groups. *Biomacromolecules* **2019**, 20, 3200–3210.
- (36) Vinciguerra, D.; Tran, J.; Nicolas, J. Telechelic Polymers from Reversible-Deactivation Radical Polymerization for Biomedical Applications. *Chem. Commun.* **2018**, *54*, 228–240.
- (37) Skrabania, K.; Kristen, J.; Laschewsky, A.; Akdemir, Ö.; Hoth, A.; Lutz, J.-F. Design, Synthesis, and Aqueous Aggregation Behavior of Nonionic Single and Multiple Thermoresponsive Polymers. *Langmuir* **2007**, 23, 84–93.
- (38) Pasparakis, G.; Manouras, T.; Vamvakaki, M.; Argitis, P. Harnessing Photochemical Internalization with Dual Degradable Nanoparticles for Combinatorial Photo-Chemotherapy. *Nat. Commun.* **2014**, *5*, 3623.
- (39) Rosen, B. M.; Jiang, X.; Wilson, C. J.; Nguyen, N. H.; Monteiro, M. J.; Percec, V. The disproportionation of Cu(I)X mediated by ligand and solvent into Cu(0) and $Cu(II)X_2$ and its implications for SET-LRP. *J. Polym. Sci., Part A: Polym. Chem.* **2009**, 47, 5606–5628.
- (40) Lutz, J.-F.; Akdemir, Ö.; Hoth, A. Point by Point Comparison of Two Thermosensitive Polymers Exhibiting a Similar LCST: Is the Age of Poly(NIPAM) Over? *J. Am. Chem. Soc.* **2006**, *128*, 13046–13047
- (41) Lutz, J. F.; Hoth, A. Preparation of Ideal PEG Analogues with a Tunable Thermosensitivity by Controlled Radical Copolymerization of 2-(2-Methoxyethoxy)ethyl Methacrylate and Oligo(ethylene glycol) Methacrylate. *Macromolecules* **2006**, *39*, 893–896.
- (42) Wang, D.; Guo, S.; Zhang, Q.; Wilson, P.; Haddleton, D. M. Mussel-Inspired Thermoresponsive Polymers with a Tunable LCST by Cu(0)-LRP for the Construction of Smart TiO₂ Nanocomposites. *Polym. Chem.* **2017**, *8*, 3679–3688.
- (43) Domingos, R. F.; Baalousha, M. A.; Ju-Nam, Y.; Reid, M. M.; Tufenkji, N.; Lead, J. R.; Leppard, G. G.; Wilkinson, K. J. Characterizing Manufactured Nanoparticles in the Environment: Multimethod Determination of Particle Sizes. *Environ. Sci. Technol.* **2009**, *43*, 7277–7284.
- (44) Zhu, J. L.; Liu, K. L.; Zhang, Z.; Zhang, X. Z.; Li, J. Amphiphilic Star-Block Copolymers and Supramolecular Transformation of Nanogel-like Micelles to Nanovesicles. *Chem. Commun.* **2011**, 47, 12849–12851.
- (45) Bhatia, S.; Mohr, A.; Mathur, D.; Parmar, V. S.; Haag, R.; Prasad, A. K. Biocatalytic Route to Sugar-PEG-Based Polymers for Drug Delivery Applications. *Biomacromolecules* **2011**, *12*, 3487–3498.
- (46) Hussain, H.; Busse, K.; Kressler, J. Poly(ethylene oxide)- and Poly(perfluorohexylethyl methacrylate)-Containing Amphiphilic Block Copolymers: Association Properties in Aqueous Solution. *Macromol. Chem. Phys.* **2003**, 204, 936–946.
- (47) Li, C.; Madsen, J.; Armes, S. P.; Lewis, A. L. A New Class of Biochemically Degradable, Stimulus-Responsive Triblock Copolymer Gelators. *Angew. Chem., Int. Ed.* **2006**, *118*, 3590–3593.
- (48) Xu, B.; Gu, G.; Feng, C.; Jiang, X.; Hu, J.; Lu, G.; Zhanga, S.; Huang, X. (PAA-g-PS)-co-PPEGMEMA Asymmetric Polymer Brushes: Synthesis, Self-Assembly, and Encapsulating Capacity for

- Both Hydrophobic and Hydrophilic Agents. Polym Chem 2016, 7, 613-624.
- (49) Cheng, X.; Jin, Y.; Fan, B.; Qi, R.; Li, H.; Fan, W. Self-Assembly of Polyurethane Phosphate Ester with Phospholipid-Like Structures: Spherical, Worm-Like Micelles, Vesicles, and Large Compound Vesicles. *ACS Macro Lett.* **2016**, *5*, 238–243.
- (50) Bao, C.; Yin, Y.; Zhang, Q. Synthesis and Assembly of Laccase-Polymer Giant Amphiphiles by Self-Catalyzed CuAAC Click Chemistry. *Biomacromolecules* **2018**, *19*, 1539–1551.
- (51) Zhang, Q.; Weber, C.; Schubert, U. S.; Hoogenboom, R. Thermoresponsive Polymers with Lower Critical Solution Temperature: from Fundamental Aspects and Measuring Techniques to Recommended Turbidimetry Conditions. *Mater. Horiz.* **2017**, 4, 109–116.
- (52) Lutz, J.-F.; Weichenhan, K.; Akdemir, Ö.; Hoth, A. About the Phase Transitions in Aqueous Solutions of Thermoresponsive Copolymers and Hydrogels Based on 2-(2-methoxyethoxy)ethyl Methacrylate and Oligo(ethylene glycol) Methacrylate. *Macromolecules* **2007**, *40*, 2503–2508.
- (53) Murthy, N.; Thng, Y. X.; Schuck, S.; Xu, M. C.; Fréchet, J. M. J. A Novel Strategy for Encapsulation and Release of Proteins: Hydrogels and Microgels with Acid-Labile Acetal Cross-Linkers. *J. Am. Chem. Soc.* **2002**, *124*, 12398–12399.
- (54) Liu, B.; Thayumanavan, S. Substituent Effects on the pH Sensitivity of Acetals and Ketals and Their Correlation with Encapsulation Stability in Polymeric Nanogels. *J. Am. Chem. Soc.* **2017**, *139*, 2306–2317.
- (55) Rodrigo, A. C.; Barnard, A.; Cooper, J.; Smith, D. K. Self-Assembling Ligands for Multivalent Nanoscale Heparin Binding. *Angew. Chem., Int. Ed.* **2011**, *50*, 4675–4679.
- (56) Concellón, A.; Blasco, E.; Martínez-Felipe, A.; Martínez, J. C.; Šics, I.; Ezquerra, T. A.; Nogales, A.; Piñol, M.; Oriol, L. Light-Responsive Self-Assembled Materials by Supramolecular Post-Functionalization via Hydrogen Bonding of Amphiphilic Block Copolymers. *Macromolecules* **2016**, *49*, 7825–7836.
- (57) Zhuang, J.; Gordon, M. R.; Ventura, J.; Li, L.; Thayumanavan, S. Multi-Stimuli Responsive Macromolecules and their Assemblies. *Chem. Soc. Rev* **2013**, *42*, 7421–7435.
- (58) Zhou, K.; Wang, Y.; Huang, X.; Luby-Phelps, K.; Sumer, B. D.; Gao, J. Tunable, Ultrasensitive pH-Responsive Nanoparticles Targeting Specific Endocytic Organelles in Living Cells. *Angew. Chem., Int. Ed.* **2011**, *50*, 6109–6114.
- (59) Hu, Y.; Darcos, V.; Monge, S.; Li, S. Synthesis and Self-Assembling of Poly(N-isopropylacrylamide-block-Poly(L -lactide)-block-Poly(N-isopropylacrylamide) Triblock Copolymers Prepared by Combination of Ring-Opening Polymerization and Atom Transfer Radical Polymerization. *J. Polym Sci. Part A Polym. Chem.* **2013**, *51*, 3274–3283.
- (60) Dai, J.; Lin, S.; Cheng, D.; Zou, S.; Shuai, X. Interlayer-crosslinked Micelle with Partially Hydrated Core Showing Reduction and pH Dual Sensitivity for Pinpointed Intracellular Drug Release. *Angew. Chem., Int. Ed.* **2011**, *50*, 9404–9408.
- (61) Hu, Q.; Sun, W.; Wang, C.; Gu, Z. Recent Advances of Cocktail Chemotherapy by Combination Drug Delivery Systems. *Adv. Drug Delivery RevAdv. Drug Deliv. Rev.* **2016**, 98, 19–34.
- (62) Bensabeh, N.; Moreno, A.; Roig, A.; Rahimzadeh, M.; Rahimi, K.; Ronda, J. C.; Cádiz, V.; Galia, M.; Percec, V.; Rodriguez-Emmenegger, C.; Lligadas, G. Photoinduced Upgrading of Lactic Acid-Based Solvents to Block Copolymer Surfactants. *ACS Sustainable Chem. Eng.* **2020**, *8*, 1276–1284.
- (63) Abdouni, Y.; Yilmaz, G.; Becer, C. R. Sequence and Architectural Control in Glycopolymer Synthesis. *Macromol. Rapid Commun* **2017**, 38, 1700212.
- (64) Miura, Y. Synthesis and Biological Application of Glycopolymers. J. Polym. Sci., Part A: Polym. Chem. 2007, 45, 5031-5036.